J Electr Eng Technol.2015;10(1): 408-421
http://dx.doi.org/10.5370/JEET.2015.10.1.408

ISSN(Print) 1975-0102
ISSN(Online) 2093-7423

PMSM Servo Drive for V-Belt Continuously Variable Transmission System Using Hybrid Recurrent Chebyshev NN Control System

Chih-Hong Lin†

Abstract – Because the wheel of V-belt continuously variable transmission (CVT) system driven by permanent magnet synchronous motor (PMSM) has much unknown nonlinear and time-varying characteristics, the better control performance design for the linear control design is a time consuming job. In order to overcome difficulties for design of the linear controllers, a hybrid recurrent Chebyshev neural network (NN) control system is proposed to control for a PMSM servo-driven V-belt CVT system under the occurrence of the lumped nonlinear load disturbances. The hybrid recurrent Chebyshev NN control system consists of an inspector control, a recurrent Chebyshev NN control with adaptive law and a recouped control. Moreover, the online parameters tuning methodology of adaptive law in the recurrent Chebyshev NN can be derived according to the Lyapunov stability theorem and the gradient descent method. Furthermore, the optimal learning rate of the parameters based on discrete-type Lyapunov function is derived to achieve fast convergence. The recurrent Chebyshev NN with fast convergence has the online learning ability to respond to the system's nonlinear and time-varying behaviors. Finally, to show the effectiveness of the proposed control scheme, comparative studies are demonstrated by experimental results.

Keywords: Permanent magnet synchronous motor, V-belt continuously variable transmission, Chebshev neural nework, Lyapunov stability

1. Introduction

A V-belt continuously variable transmission (CVT) [1-2] is typically composed of two hydraulically, or spring, actuated variable radii pulleys and a chain, or metal pushing, belt. To launch a vehicle from rest, the input pulley radius will be smaller than the output pulley radius, resulting in a speed reduction and torque multiplication transmitted to the drive shaft. For increased output shaft speed, the pulley radii are inversely manipulated simultaneously (i.e., input pulley radius increases as the output pulley radius decreases) to maintain constant belt length. A CVT may operate at a specific speed while changing the pulleys' radii to achieve torque multiplication, acceleration, and speed as per the vehicle's velocity, load requirements, engine power, and gear ratios. This operating profile provides the research motivation for CVT dynamics and nonlinear control algorithms. CVT-based vehicles have been traditionally regulated using a standard proportional integral derivative (PID)-based controller with measurements of the gear ratio [3]. It has also been demonstrated that this control strategy provides satisfactory performance using gain-scheduling with a large set of points. In addition, numerous fuzzy logic controllers [4] have also been proposed. However, V-belt continuously variable transmission (CVT) system driven by permanent magnet synchronous motor (PMSM) is yet not shown in any commercial reports so that it provides the research motivation in this study.

Since the wheel of the V-belt CVT are driven by AC motor, the selection of the AC motor drive system is a very important job. There are several types for the AC servo motors such as PMSMs, switched reluctance motors (SRMs) and induction motors (IMs). The PMSM provides higher efficiency, higher power density and lower power loss for their size compared to SRM and IM. Field-oriented control is one the most popular control technique for the PMSM servo-driven system. As a result, torque ripple can be extremely low, on par with that of SRMs and IMs. On the other hand, the PMSM controlled by field-oriented control, which can be achieved fast four-quadrant operation, are much less sensitive to the parameters variation of the motor [5-7]. The PMSM servo motor has many advantages such as high power density, high efficiency and high robustness. Therefore the PMSM has widely used in many industrial applications such as robotics and mechatronics [5-7].

Artificial neural networks (ANNs) have emerged as a powerful learning technique to perform complex tasks in highly nonlinear dynamic environments [8-15]. Some of the prime advantages of using NN are: their ability to learn based on optimization of an appropriate error function and their excellent performance for approximation of nonlinear functions. There are different paradigms of NNs proposed by different researchers for the task of system identification

† Corresponding Author: Dept. of Electrical Engineering, National United University, Miaoli 36003, Taiwan. (jhlin@nuu.edu.tw)
Received: May 1, 2014; Accepted: September 2, 2014

and control [9-11]. The models obtained with this approach are in state-space and work quite effectively in continuous-time domain. Presently, most of the NN-based system identification techniques are based on multilayer feedforward NNs or more efficient variation of this algorithm [12-15]. This is due to the fact that these networks are robust and effective in modeling and control of complex dynamic plants [12-15].

Namatame *et al*. [16] first developed Pattern classification using Chebyshev NN. Li *et al*. [17] proposed Chebyshev polynomial-based unified model NN for static function approximation. It is based on a functional link NN with Chebyshev polynomial expansion in which recursive least square learning algorithm is used. It is pointed out that this network has universal approximation capability and has faster convergence than the multilayer feedforward NN. One of the solutions for the problem of slow convergence of multilayer feedforward NN is to use some efficient learning algorithm instead of backpropagation (BP) algorithm. In this direction, the scaled complex conjugate gradient algorithm as proposed by Moeller [18] is of great importance. This algorithm chooses the search direction and the step size using information from a second order Taylor expansion of the error function. Some of the other proposals on higher order conjugate gradient algorithms are presented [19-21]. Madyastha *et al*. [22] proposed multilayer feedforward NN trained by conjugate gradient algorithm to solve data classification and function interpolation problems. However, these feedforward NNs can be used for static function approximation, but they may not be able to process dynamic behavior effectively.

The recurrent NN has received increasing attention due to its structural advantage in the modelling of the nonlinear system and dynamic control of the system [23-27]. These networks are capable of effective identification and control of complex process dynamics, but with the expense of large computational complexity. However, in the complicated nonlinear dynamic system such as the V-belt CVT system driven by PMSM with the flux linkage and external force interference is always an important factor. Hence, if each neuron in the recurrent neural networks is considered as a state in the nonlinear dynamic systems, the self-connection feedback type is able to approximate the dynamic systems efficiently [23-27]. In order to improve the ability of identifying high order systems and reduce computational complexity, the recurrent Chebyshev NN has been proposed in this study. It has more advantages than the Chebyshev NN, including better performance, higher accuracy, dynamic robustness and fast transient performance.

Due to the V-belt CVT system driven by PMSM with many nonlinear dynamics [28-30], therefore the hybrid recurrent Chebyshev NN control system is developed to ensure the control performance of robustness in this paper. The hybrid recurrent Chebyshev NN control system has fast learning property and good generalization capability. The control method can adapt to any change in the motor characteristics, which is not dependent upon the predetermined characteristics of the motor. The hybrid recurrent Chebyshev NN control system, which is composed of the inspector control, the recurrent Chebyshev NN control with adaptive law, and the recouped control, is applied to control the V-belt CVT system driven by PMSM. The online parameters training methodology of the adaptive law in the recurrent Chebyshev NN can be derived according to the Lyapunov stability theorem and the gradient descent method. The recurrent Chebyshev NN has the online learning ability to respond to the system's nonlinear and time-varying behaviors under the occurrence of the lumped nonlinear external disturbances and the parameters variation. Finally, the control performance of the proposed hybrid recurrent Chebyshev NN control system is verified by experimental results.

The paper is structured as follows: Section 2 provides the configuration of the V-belt CVT system driven by PMSM. Section 3 develops the proposed hybrid recurrent Chebyshev NN control system for controlling the V-belt CVT system driven by PMSM. Section 4 presents the simulated results for one case test and experimental results for three case studies, i.e., two kinds of speed control, and one adding load. Section 5 provides the conclusions.

2. Structure of the V-Belt CVT System Driven by PMSM

The voltage equations of the V-belt CVT system driven by PMSM in the synchronously rotating reference frame can be described as following as [5-7, 28-30]:

$$v_{qr} = R_r i_{qr} + L_{qr}\dot{i}_{qr} + \omega_f (L_{dr}\dot{i}_{dr} + \lambda_{fd}) \tag{1}$$

$$v_{dr} = R_r i_{dr} + L_{dr}\dot{i}_{dr} - \omega_f L_{qr}\dot{i}_{qr} \tag{2}$$

in which v_{qr} and v_{dr} are the *d*-axis and *q*-axis stator voltages, i_{qr} and i_{dr} are the *d*-axis and *q*-axis stator currents, L_{qr} and L_{dr} are the *d*-axis and *q*-axis stator inductances, λ_{fd} is the *d*-axis permanent magnet flux linkage, R_r is the stator resistance, ω_f is the synchronous angular speed. The electromagnetic torque T_e of the V-belt CVT system driven by PMSM can be described as [5-7, 28-30]

$$T_e = 3P_r[\lambda_{fd} i_{qr} + (L_{dr} - L_{qr}) i_{dr} i_{qr}]/4 \tag{3}$$

Then the dynamic equation of the V-belt CVT system driven by PMSM can be represented as

$$J_r\dot{\omega}_r + B_r\omega_r + T_l(T_a, \Delta T_p, F_l(B_g), \upsilon_a(v_r, B_g), \tau_a(v_r), \omega_r^2) = T_e \tag{4}$$

where $T_l(T_a, \Delta T_p, F_l(B_g), \upsilon_a(v_r, B_g), \tau_a(v_r), \omega_r^2) = T_a +$

$\Delta T_p + T_{un}$ [1-4] is the lumped nonlinear external disturbances and the parameters variation, T_a is the fixed load torque, $\Delta T_p = \Delta J_r \dot{\omega}_r + \Delta B_r \omega_r$ is the parameters variation, $T_{un} = F_l(B_g) + \upsilon_a(v_r, B_g) + \tau_a(v_r)\omega_r^2$ is the unknown nonlinear load torque, $\upsilon_a(v_r, B_g)$ is the rolling resistance, $F_l(B_g)$ is the braking force, $\tau_a(v_r)$ is the wind resistance, v_r is the total wind velocity, B_g represents the total frictional coefficient of ground surface, B_r represents the total viscous frictional coefficient and J_r is the total moment of inertia, $\omega_r = 2\omega_f / P_r$ is the rotor speed. Due to $L_{dr} = L_{qr}$ and $i_{dr} = 0$ for a surface-mounted PMSM, the second term of (3) is zero. Moreover, λ_{fd} is a constant for surface-mounted PMSM. The rotor flux is produced in the *d*-axis only, while the current vector is generated in the *q*-axis for the field-oriented control When the *d*-axis rotor flux is a constant and torque angle is $\pi/2$ [5-7], the maximum torque per ampere can be reached for the field-oriented control at the T_e proportional to the i_{qr}. The PMSM servo drive system with the implementation of field-oriented control can be reduced as

$$T_e = k_r i_{qr} \tag{5}$$

in which $k_r = 3P_r\lambda_{fd}/4$ is the torque constant. The block diagram of the V-belt CVT system driven by PMSM is shown in Fig. 1. The whole system of the V-belt CVT system driven by PMSM can be indicated as follows: a field-oriented institution, a current PI control loop, a sinusoidal PWM control circuit, an interlock circuit and an isolated circuit, an IGBT power module inverter and a torque control. In order to attain good dynamic response, all control gains for PI current loop controller are listed as follows: $k_{pc} = 10.5$ and $k_{ic} = 2.75$ through some heuristic knowledge [31-33] on the tuning of the PI controller. The field-oriented institution consists of the coordinate transformation, $\sin\theta_f / \cos\theta_f$ generation and lookup table generation. The TMS320C32 DSP control system is used to implement field-oriented institution control and speed control. The V-belt CVT system driven by PMSM is manipulated under the lumped nonlinear external disturbances.

3. Design of Hybrid Recurrent Chebyshev NN Control System

Due to much nonlinear uncertainties of the V-belt CVT system driven by PMSM such as nonlinear friction force of the transmission V-belt and clutch, these will lead to degenerate tracking response for the PMSM servo drive electric scooter. These nonlinear uncertainties cause the variation of rotor inertia and friction. For convenient design of the hybrid recurrent Chebyshev NN control system, the dynamic equation of the V-belt CVT system driven by PMSM from (4) can be rewritten as

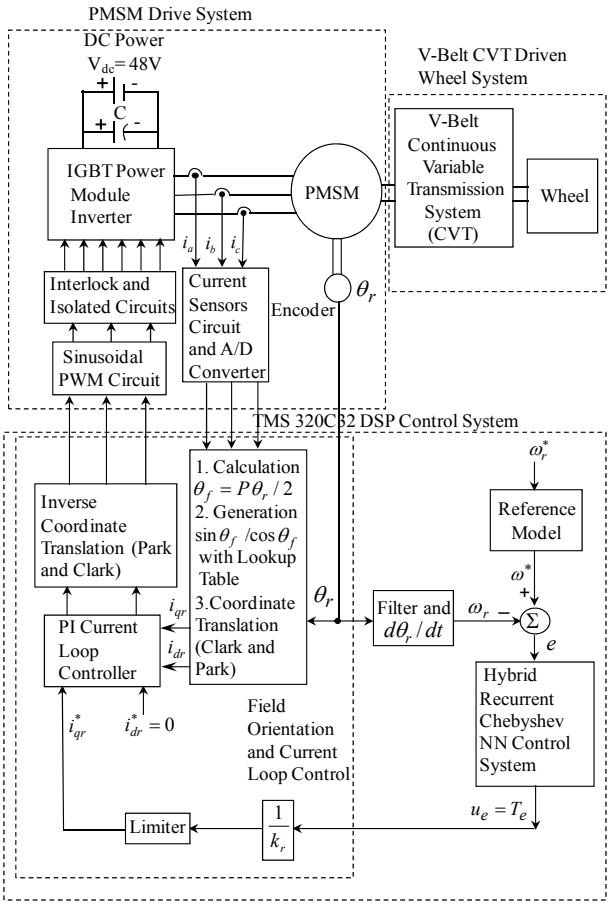

Fig. 1. Block diagram of the V-belt CVT system driven by PMSM

$$\begin{aligned}\dot{\omega}_r &= -T_l(T_{a,}\Delta T_p, F_l(B_g), \upsilon_a(v_r, B_g), \tau_a(v_r), \omega_r^2)/J_r \\ &\quad - B_r\omega_r / J_r + T_e^* / J_r \\ &= C_a T_l(T_{a,}\Delta T_p, F_l(B_g), \upsilon_a(v_r, B_g), \tau_a(v_r), \omega_r^2) \\ &\quad + A_a\omega_r + B_a u_e\end{aligned} \tag{6}$$

in which $u_e = T_e$ is the command torque of the PMSM. $A_a = -B_r / J_r$, $B_a = 1/J_r$ and $C_a = -1/J_r$ are three known constants. When the uncertainties including variation of system parameters and lumped nonlinear external disturbance occur, all parameters are assumed to be bounded, i.e., $\left|C_a T_l(T_{a,}\Delta T_p, F_l(B_g), \upsilon_a(v_r, B_g), \tau_a(v_r), \omega_r^2)\right| \le D_2$, $\left|A_a\omega_r\right| \le D_1(\omega_r)$, and $D_3 \le B_a$, where $D_1(\omega_r)$ is a known continuous function, D_2 and D_3 are two known constants. Then, the tracking error can be defined as

$$e = \omega^* - \omega_r \tag{7}$$

where ω^* represents the desired command rotor speed, e is the tracking error between the desired rotor speed and actual rotor speed. If all parameters of the V-belt CVT system driven by PMSM including variation of system

parameters and lumped nonlinear external disturbance are well known, the ideal control law can be designed as

$$u_e^* = [-C_a T_l(T_a, \Delta T_p, F_l(B_g),\ \upsilon_a(v_r, B_g), \tau_a(v_r), \omega_r^2) + \dot{\omega}^* + k_1 e - A_a \omega_r] / B_a \quad (8)$$

in which k_1 is a positive constant. Substituting (8) into (6), the error dynamic equation can be obtained

$$\dot{e} + k_1 e = 0 \quad (9)$$

The system state can track the desired trajectory gradually if $e(t) \to 0$ as $t \to \infty$ in (9). However, the novel hybrid recurrent Chebyshev NN control system is proposed to control the V-belt CVT system driven by PMSM under uncertainty perturbation. The configuration of the proposed hybrid recurrent Chebyshev NN control system is described in Fig. 2. The hybrid recurrent Chebyshev NN control system is composed of the inspector control system, the recurrent Chebyshev NN controller and the recouped controller. The control law is designed as

$$u_e = u_a + u_{rc} + u_{re} \quad (10)$$

where u_a is the proposed inspected control that capable to stabilize around a predetermined bound area in the states of the controlled system, u_{rc} is the recurrent Chebyshev NN control which is as the major tracking controller. It is used to imitate an ideal control law. The recouped control u_{re} is designed to recoup the difference between the ideal control law and the recurrent Chebyshev NN control. Since the inspected control caused the overdone and chattering effort, the recurrent Chebyshev NN control and the recouped control are proposed to reduce and smooth the control effort when the system states are inside the predetermined bound area. When the recurrent Chebyshev NN approximation properties can't be ensured, the inspected control is able to action in this case.

For the condition of divergence of states, the design of (the hybrid recurrent Chebyshev NN control system is essential to stretch the divergent states back to the predestinated bound area. The hybrid recurrent Chebyshev NN control system can uniformly approximate the ideal control law inside the bound area. Then stability of the hybrid recurrent Chebyshev NN control system can be certificated. An error dynamic equation from (6) to (10) can be rewritten as

$$\dot{e} = -k_1 e + [u_e^* - u_a - u_{rc} - u_{re}] B_a \quad (11)$$

Firstly, the inspected control u_a can be designed as

$$u_a = I_a \operatorname{sgn}(eB_a)[D_1(\omega_r) + D_2 + |\dot{\omega}^*| + |k_1 e|] / B_a \quad (12)$$

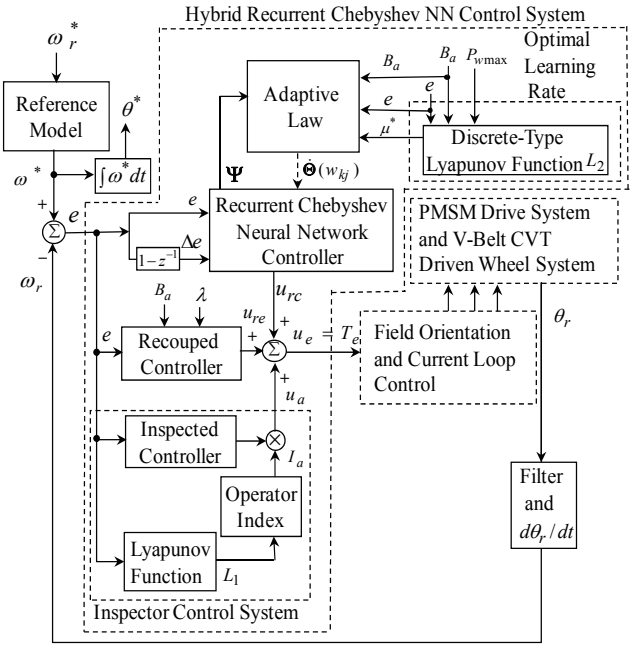

Fig. 2. Block diagram of the hybrid recurrent Chebyshev NN control system

in which $\operatorname{sgn}(\cdot)$ is a sign function. When the recurrent Chebyshev NN approximation properties can't be ensured, the inspected control law is able to action in this case, i.e., $I_a = 1$. Due to the inadequate bound values, e.g., $D_1(\omega_r)$, D_2, D_3 and sign function, the inspected control can produce in overdone and chattering effort. Therefore, the recurrent Chebyshev NN control and the recouped control can be devised to overcome the mentioned phenomenon. The recurrent Chebyshev NN control raised to imitate the ideal control u_e^*. Then the recouped control posed to recoup the difference between the ideal control u_e^* and the recurrent Chebyshev NN control u_{rc}.

Secondly, the architecture of the proposed three-layer recurrent Chebyshev NN is depicted in Fig. 3. It is composed of an input, a hidden and an output layers. The activation functions and signal actions of nodes in each layer of the recurrent Chebyshev NN can be described as follows:

3.1 First layer: Input layer

The relationship between input and output for each node *i* in this layer are expressed as

$$nod_i^1 = x_i^1(N), \quad y_i^1 = f_i^1(nod_i^1) = nod_i^1, \quad i = 1, 2 \quad (13)$$

where $x_1^1 = \omega^* - \omega_r = e$ is the tracking error between the desired speed ω^* and the rotor speed ω_r; $x_2^1 = e(1 - z^{-1}) = \Delta e$ is the tracking error change; *N* denotes the number of iterations; f_j^2 is the activation function which is selected as a linear function; y_i^1 is the output value of the input layer in the recurrent Chebyshev NN.

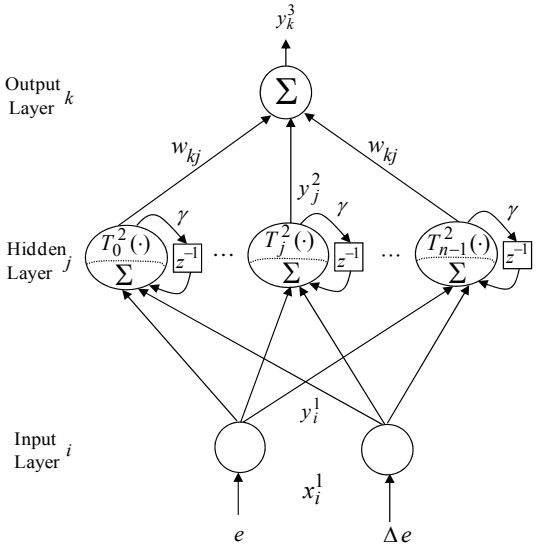

Fig. 3. Structure of the three-layer recurrent Chebyshev NN

3.2 Second layer: Hidden layer

The single node *j*th in this layer is labeled with $\sum$. The net input and the net output for node *j*th of the hidden layer are expressed as

$$\begin{aligned} nod_j^2(N) &= \sum_{i=1}^{2} y_i^1(N) + \gamma\, y_j^2(N-1), \\ y_j^2(N) &= f_j^2(nod_j^2(N)) \\ &= T_j^2(nod_j^2(N)),\ j = 0,\ 1,\ \cdots,\ n-1 \end{aligned} \tag{14}$$

where $T_j^2(\cdot)$ is the Chebyshev polynomial [16-17] which is selected as activation function of the hidden layer; y_j^2 is the output value of the hidden layer; f_j^2 is the activation function which is selected as Chebyshev polynomial; n is the number of neurons in the hidden layer; γ is the self-connecting feedback gain of the hidden layer which is selected between 0 and 1. The first few Chebyshev polynomials are given by $T_0^2(x) = 1$, $T_1^2(x) = x$ and $T_2^2(x) = 2x^2 - 1$. The higher order Chebyshev polynomials may be generated by the recursive formula given by $T_{n+1}^2(x) = 2xT_n^2(x) - T_{n-1}^2(x)$.

3.3 Third layer: Output layer

The single node *k*th in this layer is labeled with $\sum$. It computes the overall output as the summation of all input signals. The net input and the net output for node *k*th in this layer are expressed as

$$\begin{aligned} nod_k^3(N) &= \sum_{j=0}^{2} w_{kj} y_j^2(N), \\ y_k^3(N) &= f_k^3(nod_k^3(N)) = nod_k^3(N), \quad k = 1 \end{aligned} \tag{15}$$

where w_{kj} is the connective weight between the hidden layer and the output layer; f_k^3 is the activation function which is selected as a linear function; $x_j^3(N) = y_j^2(N)$ represents the *j*th input to the node of output layer. The output value of the recurrent Chebyshev NN can be represented as $y_k^3(N) = u_{rc}$, and the output value of the recurrent Chebyshev NN can also be denoted as

$$u_{rc} = \Theta^T \Psi \tag{16}$$

in which $\Theta = \left[w_{10}\ w_{11} \cdots w_{1,\,n-1} \right]^T$ is the adjustable weight parameters vector between the hidden layer and the output layer of the recurrent Chebyshev NN. $\Psi = \left[x_0^3\ x_1^3 \cdots x_{n-1}^3 \right]^T$ is the inputs vector in the output layer of the recurrent Chebyshev NN, in which x_j^3 is determined by the selected Chebyshev polynomials.

Thirdly, in order to evolve the recouped control u_{re}, a minimum approximation error δ is defined as

$$\delta = u_e^* - u_{rc}^* = u_e^* - (\Theta^*)^T \Psi \tag{17}$$

in which Θ^* is an ideal weight vector to reach of minimum approximation error. It is assumed that absolute value of δ is less than a small positive value λ, i.e., $|\delta| < \lambda$. Then, the error dynamic equation from (11) can be rewritten as

$$\begin{aligned} \dot{e} &= -k_1 e + [(u_e^* - u_{rc}) - u_{re} - u_a] B_a \\ &= -k_1 e + [(u_e^* - u_{rc}^* + u_{rc}^* - u_{rc}) - u_{re} - u_a] B_a \\ &= -k_1 e + [(u_e^* - u_{rc}^*) + (\Theta^*)^T \Psi - (\Theta)^T \Psi) - u_{re} - u_a] B_a \\ &= -k_1 e + [\delta + (\Theta^* - \Theta)^T \Psi - u_{re} - u_a] B_a \end{aligned} \tag{18}$$

Then, the Lyapunov function is selected as

$$L_1(t) = e^2 / 2 + (\Theta^* - \Theta)^T (\Theta^* - \Theta) / (2\mu) \tag{19}$$

in which μ is the learning rate. Differentiating the Lyapunov function with respect to *t* and using (18), then (19) can be rewritten as

$$\begin{aligned} \dot{L}_1(t) &= \dot{e}e - (\Theta^* - \Theta)^T \dot{\Theta} / \mu \\ &= \{-k_1 e + [\delta - u_{re} - u_a] B_a\} e \\ &\quad + (\Theta^* - \Theta)^T \Psi B_a e - (\Theta^* - \Theta)^T \dot{\Theta} / \mu \end{aligned} \tag{20}$$

In order to $\dot{L}_1 \le 0$, the adaptive law $\dot{\Theta}$ and the recouped controller u_{re} can be designed as follow as

$$\dot{\Theta} = \mu \Psi B_a e \tag{21}$$

$$u_{re} = \lambda \operatorname{sgn}(B_a e) \tag{22}$$

in which $\lambda > 0$ is an adaptive gain. In order to avoid

chattering phenomenon of sliding mode, the sign function $\mathrm{sgn}(B_a e_c)$ can be replaced by the equation $B_a e_c / (|B_a e_c| + \rho)$, where $\rho = \begin{cases} \rho_0, & |B_a e_c| < \eta \\ 0, & |B_a e_c| \geq \eta \end{cases}$, ρ_0 and η are positive constants. Substituting (21) and (12) into (20) and using (12) with $I_a = 0$, then (20) can be represented as

$$\dot{L}_1(t) = -k_1 e^2 + (\delta - u_{re} - u_a) B_a e \leq -k_1 e^2 + (\delta - u_{re}) B_a e \tag{23}$$

From (22), then (23) can be obtained as

$$\begin{aligned} \dot{L}_1(t) &\leq -k_1 e^2 + \{\delta - u_{re}\} B_a e \leq -k_1 e^2 + \{|\delta| - \lambda\} |B_a e| \\ &\leq -k_1 e^2 \leq 0 \end{aligned} \tag{24}$$

From (24), the $\dot{L}_1(t)$ is a negative semi-definite, i.e. $L_1(t) \leq L_1(0)$. It implies that e and $(\Theta^* - \Theta)$ be bounded. Furthermore, the function is defined as

$$\varepsilon(t) = -\dot{L}_1(t) = k_1 e^2 \tag{25}$$

Integrating (25) with respect to *t*, then

$$\int_0^t \varepsilon(\tau) d\tau = \int_0^t [-\dot{L}_1(t)] dt = L_1(0) - L_1(t) \tag{26}$$

Due to $L_1(0)$ is bounded, and $L_1(t)$ is nonincreasing and bounded, then

$$\lim_{t \to \infty} \int_0^t \varepsilon(\tau) d\tau < \infty \tag{27}$$

Differentiating (25) with respect to *t* gives

$$\dot{\varepsilon}(t) = 2 k_1 e \dot{e} \tag{28}$$

Due to all the variables in the right side of (18) are bounded. It implies that $\dot{e}$ is also bounded. Then, $\varepsilon(t)$ is a uniformly continuous function [34-35]. It is denoted that $\lim_{t \to \infty} \varepsilon(t) = 0$ by using Barbalat's lemma [34-35]. Therefore $e(t) \to 0$ as $t \to \infty$. From above proof, the hybrid recurrent Chebyshev NN control system is gradually stable.

According to Lyapunov stability theorem and the gradient descent method, an online parameter training methodology of the recurrent Chebyshev NN can be derived and trained effectively. Then the parameter of adaptation law $\dot{\Theta}(w_{kj})$ shown in (21) can be rewritten as

$$\dot{w}_{kj} = \mu x_j^3 B_a e \tag{29}$$

Using the gradient descent method, the adaptive law $\dot{\Theta}(w_{kj})$ also can be represented as

$$\dot{w}_{kj} = -\mu \frac{\partial L_1}{\partial w_{kj}} = -\mu \frac{\partial L_1}{\partial y_k^3} \frac{\partial y_k^3}{\partial nod_k^3} \frac{\partial nod_k^3}{\partial w_{kj}^3} = -\mu \frac{\partial L_1}{\partial y_k^3} x_j^3 \tag{30}$$

Comparing (29) with (31), the above Jacobian term of control system can be rewritten as

$$\partial L_1 / \partial y_k^3 = -e B_a \tag{31}$$

The adaptive law $\dot{\Theta}(w_{kj})$ shown in (21) calls for a proper choice of the learning rate. For a small value of learning rate, the convergence of controller parameter can be guaranteed but the convergent speed is very slow. In order to train the recurrent Chebyshev NN efficiently, an optimal learning rate will be derived to achieve the fast convergence of output tracking error. Then, the convergence analysis in the following theorem is to derive specific learning rate to assure convergence of the output tracking error.

Theorem 1: Let μ be the learning rate of the recurrent Chebyshev NN weights, and let $P_{w\max}$ be defined as $P_{w\max} \equiv max_N \|P_w(N)\|$, where $P_w(N) = \partial y_k^3 / \partial w_{kj}$ and $\|\cdot\|$ is the Euclidean norm in $\Re^n$. Then, the convergence of the output tracking error is guaranteed if is chosen as

$$0 < \mu < \frac{2}{(P_{w\max})^2 [eB_a / e(N)]^2} \tag{32}$$

Moreover, the optimal learning rate which achieves the fast convergence can be obtained as

$$\mu^* = 1 / [(P_{w\max})^2 [eB_a / e(N)]^2] \tag{33}$$

Proof: Since

$$P_w(N) = \frac{\partial y_k^3}{\partial w_{kj}} = x_j^3 \tag{34}$$

Then, a discrete-type Lyapunov function is selected as

$$L_2(N) = \frac{1}{2} e^2(N) \tag{35}$$

The change in the Lyapunov function is obtained by

$$\Delta L_2(N) = L_2(N+1) - L_2(N) = \frac{1}{2} \left[e^2(N+1) - e^2(N) \right] \tag{36}$$

The error difference can be represented by

$$e(N+1)=e(N)+\Delta e(N)=e(N)+\left[\frac{\partial e(N)}{\partial w_{kj}}\right]^T \Delta w_{kj} \quad (37)$$

where $\Delta e(N)$ is the output error change Δw_{kj} represents change of the weight. Using (29), (30), (31) and (34), then (37) can be obtained

$$\frac{\partial e(N)}{\partial w_{kj}}=\frac{\partial e(N)}{\partial L_1}\frac{\partial L_1}{\partial y_k^3}\frac{\partial y_k^3}{\partial w_{kj}}=-\frac{eB_a}{e(N)}P_w(N) \quad (38)$$

$$e(N+1)=e(N)-\left[\frac{eB_a}{e(N)}P_w(N)\right]^T \mu eB_a P_w(N) \quad (39)$$

Thus

$$\begin{aligned}\left\|e(N+1)\right\| &= \left\|e(N)\left[1-\mu\left(eB_a/e(N)\right)^2 P_w^T(N)P_w(N)\right]\right\| \\ &\le \left\|e(N)\right\|\left\|1-\mu\left(eB_a/e(N)\right)^2 P_w^T(N)P_w(N)\right\| \end{aligned} \quad (40)$$

From (36) to (40), $\Delta L_2(N)$ can be rewritten as

$$\begin{aligned}\Delta L_2(N) &= \frac{1}{2}\mu\left[eB_a\right]^2 P_w^T(N)P_w(N) \\ &\quad\cdot\left\{\mu\left[eB_a/e(N)\right]^2 P_w^T(N)P_w(N)-2\right\} \\ &\le \frac{1}{2}\mu\left[eB_a\right]^2\left(P_{w\max}(N)\right)^2 \\ &\quad\cdot\left\{\mu\left[eB_a/e(N)\right]^2\left(P_{w\max}(N)\right)^2-2\right\}\end{aligned} \quad (41)$$

If μ is chosen as $0<\mu<2/\{(P_{w\max})^2[eB_a/e(N)]^2\}$, then the Lyapunov stability of $L_2(N)>0$ and $\Delta L_2<0$ is guaranteed so that the output tracking error will converge to zero as $t\to 0$. This completes the proof of the theorem. Moreover, the optimal learning-rate which achieves the fast convergence is corresponding to

$$2\mu^*\{(P_{w\max})^2[eB_a/e(N)]^2\}-2=0 \quad (42)$$

i.e.,

$$\mu^*=1/\{(P_{w\max})^2[eB_a/e(N)]^2\} \quad (43)$$

which comes from the derivative of (41) with respect to μ and equals to zero. This shows an interesting result for the variable optimal learning rate which can be online tuned at each instant. In summary, the online learning algorithm of the recurrent Chebyshev NN controller is based on the adaptive law (29) for the weight adjustment with the optimal learning rate in (33).

4. Simulated and Experimental Results

The whole system of the DSP-based control system for the V-belt CVT system driven by PMSM is shown in Fig. 1. The control algorithm was executed by a TMS320C32 DSP control system including multi-channels of D/A, eight channels of programmable PWM and an encoder interface circuit. The IGBT power module voltage source inverter is executed by current-controlled sinusoidal PWM with a switching frequency of 15 *k*Hz. The current PID loop controller is the current loop tracking controller. The specification of the used PMSM is a three-phase 48V, 750W, 16.5A, 3600*rpm*. The parameters of the PMSM are listed as: $R_r=2.5\Omega$, $L_{dr}=L_{qr}=6.53$ *mH*, $\overline{J}_r=62.15\times10^{-3}$ *Nms*, $\overline{B}_r=6.18\times10^{-3}$ *Nms/rad*, $k_r=0.86$ Nm/A by means of open circuit test, short test, rotor block test, loading test.

In order to comparison the control performance of the proposed recurrent Chebyshev NN control system and the PI controller, one simulation test and three experimentation tests are provided. Since the electric scooter is a nonlinear and time-varying system, two gains of the PI controller are $k_{ps}=18.2$ and $k_{is}=5.6$ through some heuristic knowledge [31-33] on the tuning of the PI controller in order to achieve good transient and steady-state control performance at 157 *rad/s* case under the lumped nonlinear external disturbances with parameters variation $T_l=\Delta T_p+T_{un}$ by experimental test. Furthermore, the control gains of the proposed hybrid recurrent Chebyshev NN control system are selected as $\gamma=0.1$, $\lambda=0.6$. Usually, some heuristics can be used to roughly initialize the parameters of the recurrent Chebyshev NN for practical application. The effect due to the inaccurate selection of the initialized parameters can be retrieved by the online parameters training methodology. For simplicity, all connective weights between hidden layer and output layer in the recurrent Chebyshev NN are initialized with random number. Furthermore, the normalized inputs and references have zero and unity, respectively. Also the network outputs should be converted back to the original unit of the references. The parameter adjustment process remains continually active for the duration of the experimentation. Accurate tracking control performance for the V-belt CVT system driven by PMSM can be obtained after one cycle of online training of the recurrent Chebyshev NN. The structure of recurrent Chebyshev NN controller has 2 nodes, 3 nodes and 1 node in the input layer, the hidden layer and the output layer, respectively.

4.1 Simulated results

The simulated test is provided at 314 *rad/s* with adding load torque disturbance $T_l=2Nm$ in $t=1.2$ sec case. The simulated results of the PI controller and the hybrid recurrent Chebyshev NN control system for the V-belt CVT driven electric scooter by using the PMSM servo

drive system at 314 rad/s with adding load torque disturbance $T_l = 2Nm$ in $t = 1.2$ sec are shown in Figs. 4, 5, 6 and Figs. 7-9, respectively. The speed responses of the PI controller and the hybrid recurrent Chebyshev NN control system are shown in Figs. 5 and 7, respectively. The zoom errors of speed of the PI controller and the hybrid recurrent Chebyshev NN control system are shown in Figs. 6 and 8, respectively. The electromagnetic torques of the PI controller and the hybrid recurrent Chebyshev NN control system are shown in Figs. 7 and 9, respectively.

The hybrid recurrent Chebyshev NN control system has smaller error of speed, better load regulation and smaller torque ripple than the PI controller due to online adaptive mechanism of recurrent Chebyshev NN with fast convergence and action of the recouped controller. In addition, the hybrid recurrent Chebyshev Legendre NN control system has faster dynamic response and faster convergence from the response of the optimal learning rate μ^* of connective weights in the recurrent Chebyshev NN at 314 *rad/s* with adding load torque disturbance $T_l = 2Nm$ in $t = 1.2$ sec shown in Fig. 10.

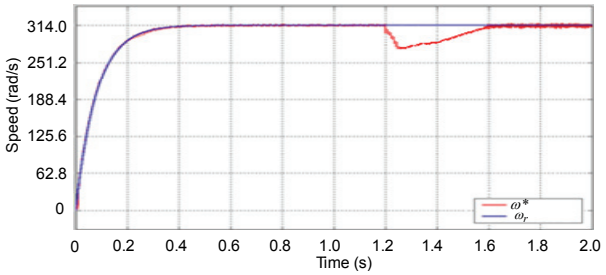

Fig. 4. Simulated result of speed tracking response using the PI controller for the V-belt CVT system driven by PMSM at 314 *rad/s* case with adding load torque disturbance $T_l = 2Nm$ in t=1.2sec

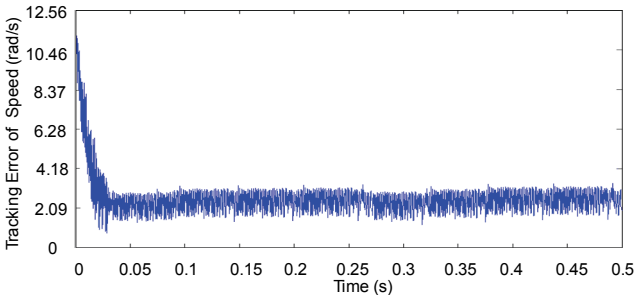

Fig. 5. Simulated results of speed tracking error using the PI controller for the V-belt CVT system driven by PMSM at 314 *rad/s* case with adding load torque disturbance $T_l = 2Nm$ in t=1.2sec

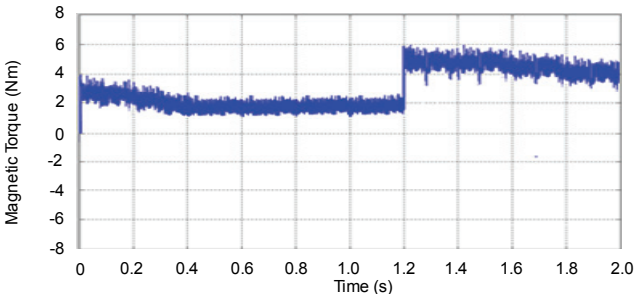

Fig. 6. Simulated result of command electromagnetic torque response using the PI controller for the V-belt CVT system driven by PMSM at 314 *rad/s* case with adding load torque disturbance $T_l = 2Nm$ in t=1.2sec

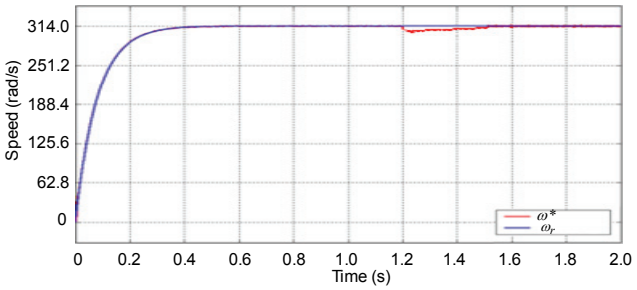

Fig. 7. Simulated result of speed tracking response using the hybrid recurrent Chebyshev NN control system for the V-belt CVT system driven by PMSM at 314 *rad/s* case with adding load torque disturbance $T_l = 2Nm$ in t=1.2sec

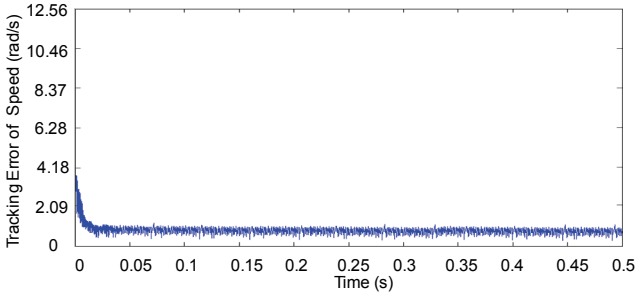

Fig. 8. Simulated results of speed tracking error using the hybrid recurrent Chebyshev NN control system for the V-belt CVT system driven by PMSM at 314 *rad/s* case with adding load torque disturbance $T_l = 2Nm$ in t=1.2sec

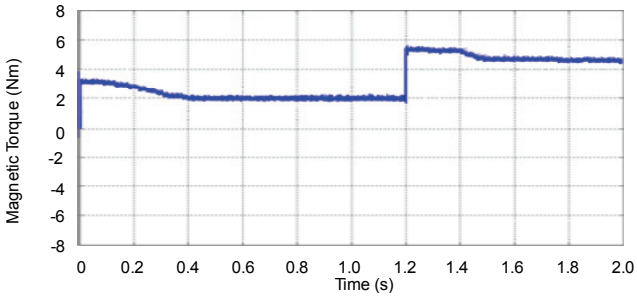

Fig. 9. Simulated result of command electromagnetic torque response using the hybrid recurrent Chebyshev NN control system for the V-belt CVT system driven by PMSM at 314 *rad/s* case with adding load torque disturbance $T_l = 2Nm$ in t=1.2sec

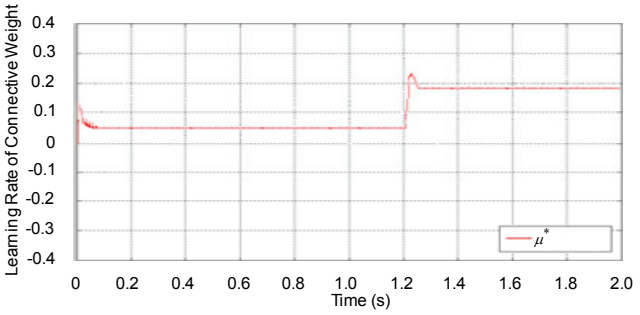

Fig. 10. Simulated results of learning rate μ^* of connective weights in the recurrent Chebyshev NN at 314 *rad/s* with adding load torque disturbance T_l= 2*Nm* in t=1.2sec

4.2 Experimental results

Two experimental tests are provided at 157 *rad/s* case under the smaller lumped external disturbances with parameters variation $T_l = \Delta T_p + T_{un}$ and 314 *rad/s* case under the lager lumped external disturbances with twice parameters variation $T_l = 2\Delta T_p + T_{un}$. Firstly, the experimental results of the PI controller for the V-belt CVT driven electric scooter by using the PMSM servo drive system at 157 *rad/s* case and 314 *rad/s* case are shown in Figs. 11-14 and Figs. 15-18, respectively. The speed tracking response of command rotor speed ω_r^*, desired command rotor speed ω^* and measured rotor speed ω_r using the PI controller for the V-belt CVT system driven by PMSM at 157 *rad/s* case is shown in Fig. 11. The response of speed tracking error e using the PI controller for the V-belt CVT system driven by PMSM at 157 *rad/s* case is shown in Fig. 12. The response of speed tracking error e amplification using the PI controller for the V-belt CVT system driven by PMSM at 157 *rad/s* case is shown in Fig. 13. The response of command electromagnetic torque T_e using the PI controller for the V-belt CVT system driven by PMSM at 157 *rad/s* case is shown in Fig. 14. The speed tracking response of command rotor speed ω_r^*, desired command rotor speed ω^* and measured rotor speed ω_r using the PI controller for the V-belt CVT system driven by PMSM at 314 *rad/s* case is shown in Fig. 15. The response of speed tracking error e using the PI controller for the V-belt CVT system driven by PMSM at 314 *rad/s* case is shown in Fig. 16. The response of speed tracking error e amplification using the PI controller for the V-belt CVT system driven by PMSM at 314 *rad/s* case is shown in Fig.

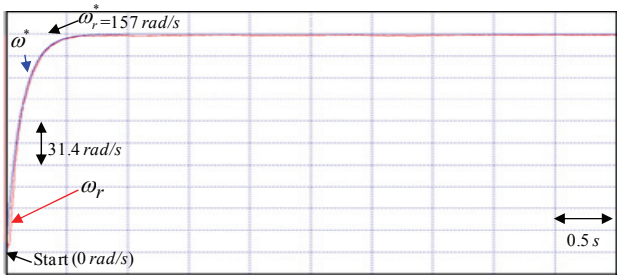

Fig. 11. Experimental result of speed tracking response using the PI controller for the V-belt CVT system driven by PMSM at 157 *rad/s* case

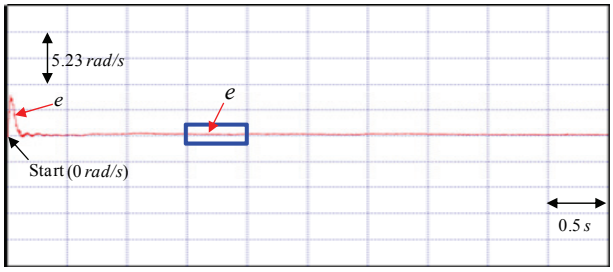

Fig. 12. Experimental result of speed tracking error using the PI controller for the V-belt CVT system driven by PMSM at 157 *rad/s* case

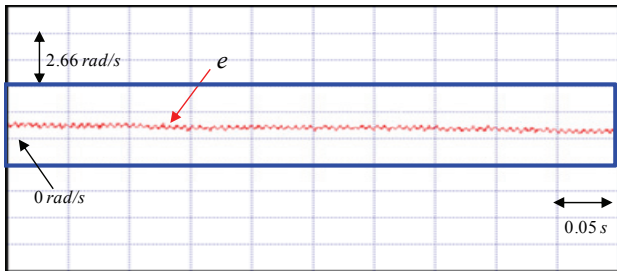

Fig. 13. Experimental result of speed tracking error amplification using the PI controller for the V-belt CVT system driven by PMSM at 157 *rad/s* case

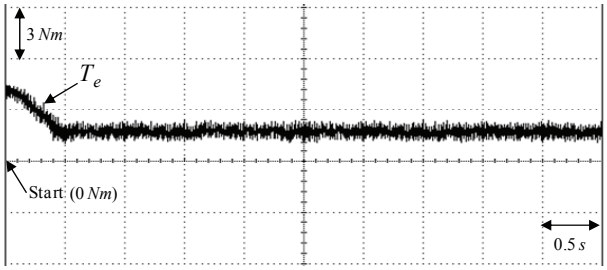

Fig. 14. Experimental result of command electromagnetic torque response using the PI controller for the V-belt CVT system driven by PMSM at 157 *rad/s* case

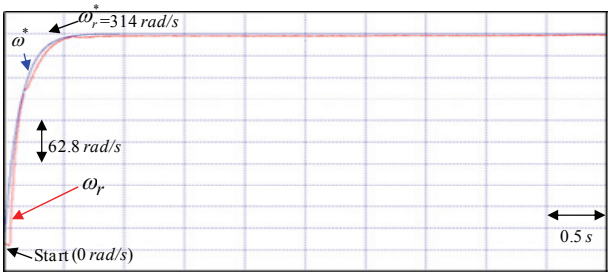

Fig. 15. Experimental result of speed tracking response using the PI controller for the V-belt CVT system driven by PMSM at 314 *rad/s* case

17. The response of command electromagnetic torque T_e using the PI controller for the V-belt CVT system driven by PMSM at 314 *rad/s* case is shown in Fig. 18.

Since the low speed operation is the same as the nominal case due to smaller disturbance, the responses of speed shown in Fig. 11 has better tracking performance. Moreover, the degenerate tracking response of speed shown in Fig. 15 is very obvious under the bigger nonlinear disturbances (e.g. rolling resistance, parameters variation) at high speed perturbation. In addition, the command electromagnetic torque brings in greater torque ripple shown in Figs. 14 and Fig. 18. From the experimental results, sluggish tracking responses of speed is obtained for the V-belt CVT system driven by PMSM using the PI controller. The linear controller has the weak robustness under the bigger nonlinear disturbances because of no appropriately gains tuning or no degenerate nonlinear effect.

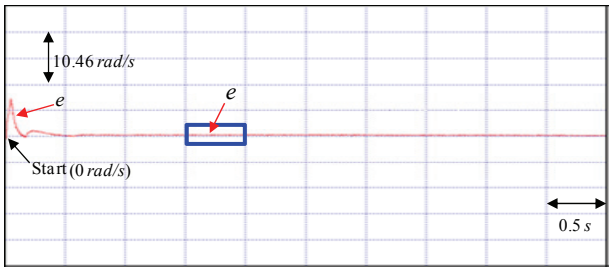

Fig. 16. Experimental result of speed tracking error using the PI controller for the V-belt CVT system driven by PMSM at 314 *rad/s* case

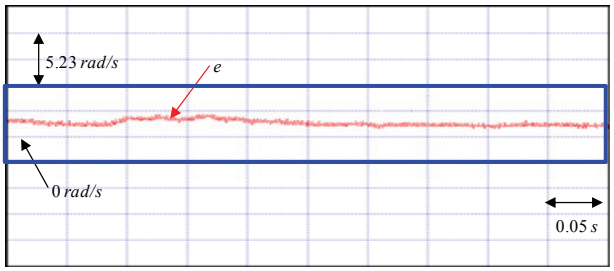

Fig. 17. Experimental result of speed tracking error amplification using the PI controller for the V-belt CVT system driven by PMSM at 314 *rad/s* case

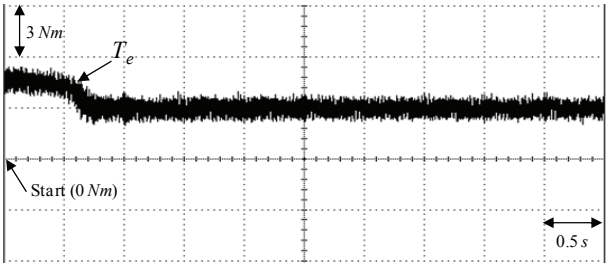

Fig. 18. Experimental result of command electromagnetic torque response using the PI controller for the V-belt CVT system driven by PMSM at 314 *rad/s* case

In addition, the experimental results of the hybrid recurrent Chebyshev NN control system for the V-belt CVT system driven by PMSM at 157 *rad/s* case and 314 *rad/s* case are shown in Figs. 19-22 and Figs. 23-26, respectively. The speed tracking response of command rotor speed ω_r^*, desired command rotor speed ω^* and measured rotor speed ω_r using the hybrid recurrent Chebyshev NN control system for the V-belt CVT system driven by PMSM at 157 *rad/s* case is shown in Fig. 19. The response of speed tracking error e using the hybrid recurrent Chebyshev NN control system for the V-belt CVT system driven by PMSM at 157 *rad/s* case is shown in Fig. 20. The response of speed tracking error e amplification using the hybrid recurrent Chebyshev NN

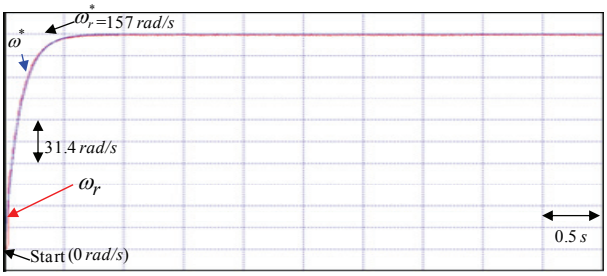

Fig. 19. Experimental result of speed tracking response using the hybrid recurrent Chebyshev NN control system for the V-belt CVT system driven by PMSM at 157 *rad/s* case

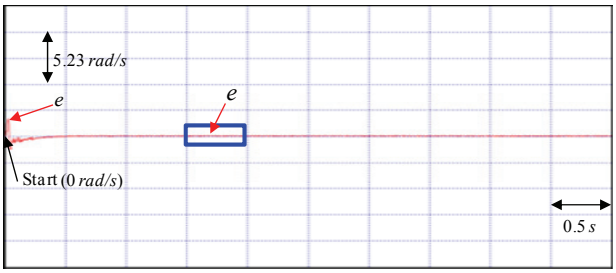

Fig. 20. Experimental result of speed tracking error using the hybrid recurrent Chebyshev NN control system for the V-belt CVT system driven by PMSM at 157 *rad/s* case

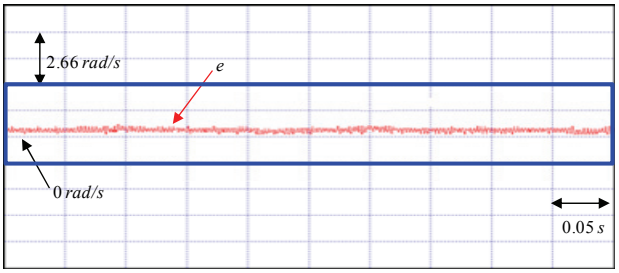

Fig. 21. Experimental result of speed tracking error amplification using the hybrid recurrent Chebyshev NN control system for the V-belt CVT system driven by PMSM at 157 *rad/s* case

control system for the V-belt CVT system driven by PMSM at 157 *rad/s* case is shown in Fig. 21. The response of command electromagnetic torque T_e using the hybrid recurrent Chebyshev NN control system for the V-belt CVT system driven by PMSM at 157 *rad/s* case is shown in Fig. 22. The speed tracking response of command rotor speed ω_r^*, desired command rotor speed ω^* and measured rotor speed ω_r using the hybrid recurrent Chebyshev NN control system for the V-belt CVT system driven by PMSM at 314 *rad/s* case is shown in Fig. 23. The response of speed tracking error *e* using the hybrid recurrent Chebyshev NN control system for the V-belt CVT system driven by PMSM at 314 *rad/s* case is shown in Fig. 24. The response of speed tracking error e amplification using the hybrid recurrent Chebyshev NN control system for the V-belt CVT system driven by PMSM at 314 *rad/s* case is shown in Fig. 25. The response of command electromagnetic torque T_e using the hybrid recurrent Chebyshev NN control system for the V-belt CVT system driven by PMSM at 314 *rad/s* case is shown in Fig. 26.

However, owing to the online adaptive mechanism of recurrent Chebyshev NN and the recouped controller, accurate tracking control performance of the V-belt CVT system driven by PMSM can be obtained. These results show that the hybrid recurrent Chebyshev NN control system has better performance than the PI controller for the V-belt CVT system driven by PMSM at high speed perturbation under the lumped nonlinear external disturbances with twice parameters variation. Additionally, the

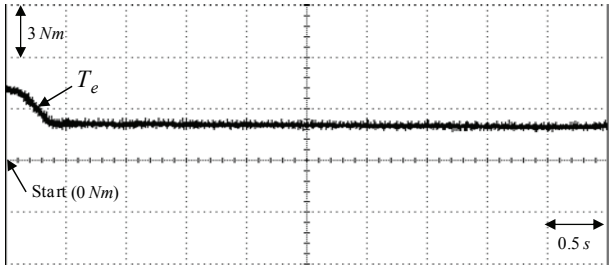

Fig. 22. Experimental result of command electromagnetic torque response using the hybrid recurrent Chebyshev NN control system for the V-belt CVT system driven by PMSM at 157 *rad/s* case

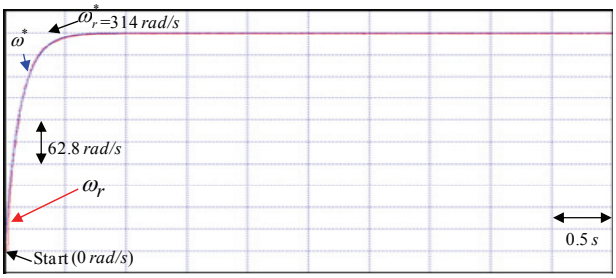

Fig. 23. Experimental result of speed tracking response using the hybrid recurrent Chebyshev NN control system for the V-belt CVT system driven by PMSM at 314 *rad/s* case

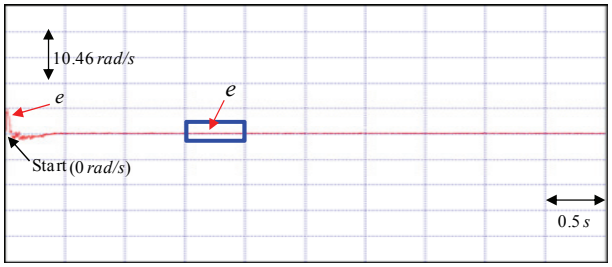

Fig. 24. Experimental result of speed tracking error using the hybrid recurrent Chebyshev NN control system for the V-belt CVT system driven by PMSM at 314 *rad/s* case

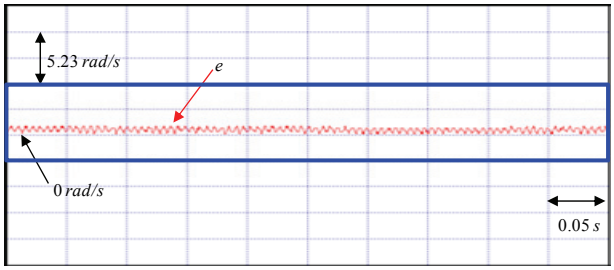

Fig. 25. Experimental result of speed tracking error amplification using the hybrid recurrent Chebyshev NN control system for the V-belt CVT system driven by PMSM at 314 *rad/s* case

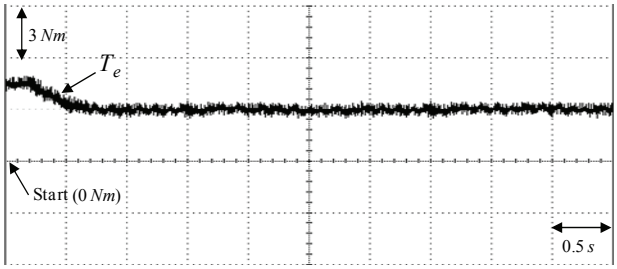

Fig. 26. Experimental result of command electromagnetic torque response using the hybrid recurrent Chebyshev NN control system for the V-belt CVT system driven by PMSM at 314 *rad/s* case

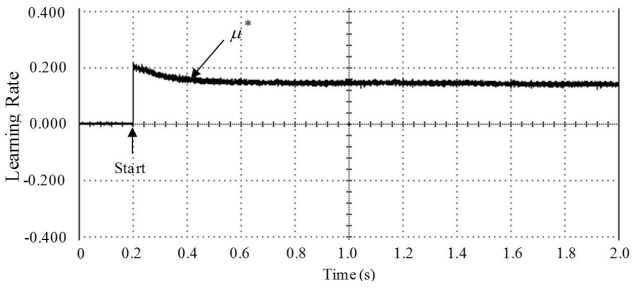

Fig. 27. Experimental result of optimal learning rate μ^* of connective weights in the recurrent Chebyshev NN at 157 *rad/s* case

small chattering phenomenon of the electromagnetic torque shown in Fig. 26 is induced by online adjustment of the recurrent Chebyshev NN to cope with high-frequency unmodelled dynamics of plant. Moreover, the dynamic response of command electromagnetic torque T_e shown in Fig. 22 and Fig. 26 by using the hybrid recurrent Chebyshev NN control system has lower torque ripple than by using the PI controller shown in Figs. 14 and Fig. 18. In addition, the recurrent Chebyshev NN control system has faster dynamic response and faster convergence from the responses of the optimal learning rate of connective weights in the recurrent Chebyshev NN control at 157 *rad/s* case and 314 *rad/s* case shown in Figs. 27 and 28, respectively.

The measured rotor speed response under step disturbance torque is given finally. The PI control and the hybrid recurrent Chebyshev NN control system are tested under T_l=2*Nm* (T_a)+T_{un} load torque disturbances with adding load. The experimental result of the measured rotor speed responses using the PI controller under T_l=2*Nm* (T_a)+T_{un} load torque disturbances with adding load at 314 *rad/s* is shown in Fig. 29. The experimental result of the measured current i_a in phase *a* using the PI controller under T_l=2*Nm* (T_a)+T_{un} load torque disturbances with adding load at 314 *rad/s* is shown in Fig. 30.

The experimental result of the measured rotor speed responses using the hybrid recurrent Chebyshev NN control system under T_l=2*Nm* (T_a)+T_{un} load torque disturbances with adding load at 314 *rad/s* is shown in Fig. 31. The experimental result of the measured current i_a in phase *a* using the hybrid recurrent Chebyshev NN control system under T_l=2*Nm* (T_a)+T_{un} load torque disturbances with adding load at 314 *rad/s* is shown in Fig. 32.

From the experimental results, the degenerated responses under T_l=2*Nm* (T_a)+T_{un} load torque disturbances are much improved using the hybrid recurrent Chebyshev NN control system. From experimental results, transient response of the hybrid recurrent Chebyshev NN control system is better than PI controller at load regulation. In addition, the control performance comparisons of the PI controller and hybrid recurrent Chebyshev NN control system are summarized in Table 1 for experimental results at three test cases. In Table 1, the hybrid recurrent

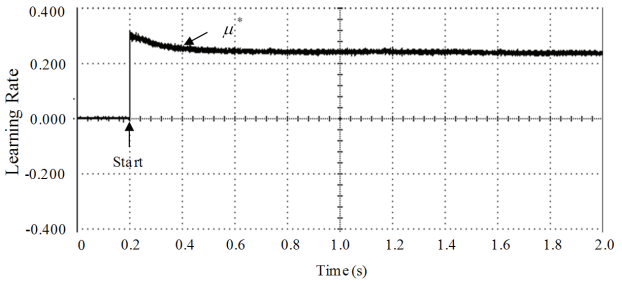

Fig. 28. Experimental result of optimal learning rate μ^* of connective weights in the recurrent Chebyshev NN at 314 *rad/s* case

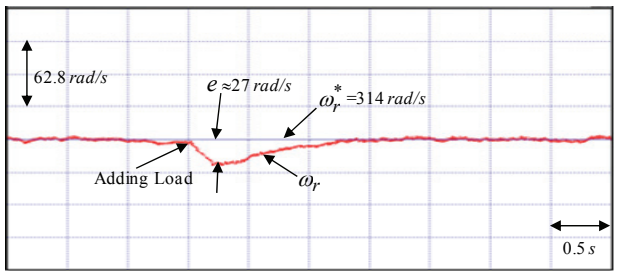

Fig. 29. Experimental result of speed response using the PI controller under T_l=2*Nm* (T_a)+T_{un} load torque disturbances with adding load at 314 *rad/s* case

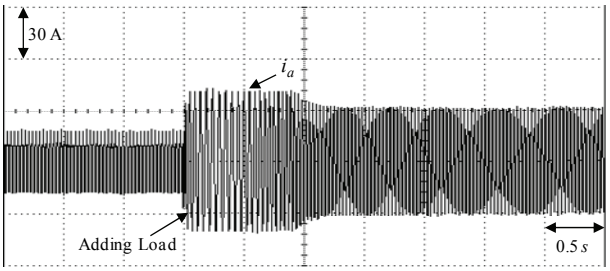

Fig. 30. Experimental result of measured current in phase *a* using the PI controller under T_l=2*Nm* (T_a)+T_{un} load torque disturbances with adding load at 314 *rad/s* case

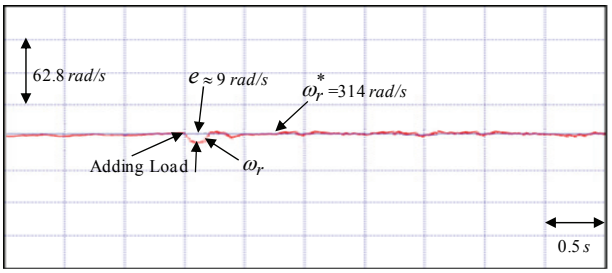

Fig. 31. Experimental result of speed response using the hybrid recurrent Chebyshev NN control system under T_l=2*Nm* (T_a)+T_{un} load torque disturbances with adding load at 314 *rad/s* case

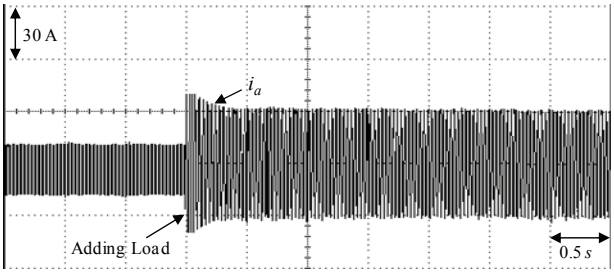

Fig. 32. Experimental result of measured current in phase a using the hybrid recurrent Chebyshev NN control system under T_l=2*Nm* (T_a)+T_{un} load torque disturbances with adding load at 314 *rad/s* case

Table 1. Performance comparison of control systems

Control system and three test cases / Performance	PI controller		
	157*rad/s* case under the lumped nonlinear external disturbances with parameters variation $T_l = \Delta T_p + T_{un}$	314*rad/s* caseunder the lumped nonlinear external disturbances with twiceparameters variation $T_l = 2\Delta T_p + T_{un}$	With adding load under $T_l = 2Nm\ (T_a) + T_{un}$ load torque disturbances
Max. error of *e*	4.2 *rad/s*	8.4 *rad/s*	27 *rad/s*
RMS error of *e*	0.8 *rad/s*	2.1 *rad/s*	4.1 *rad/s*
Control system and three test cases / Performance	Hybrid recurrent chebyshev NN control system		
	157*rad/s* case under the lumped nonlinear external disturbances with parameters variation $T_l = \Delta T_p + T_{un}$	314*rad/s* caseunder the lumped nonlinear external disturbances with twiceparameters variation $T_l = 2\Delta T_p + T_{un}$	With adding load under $T_l = 2Nm\ (T_a) + T_{un}$ load torque disturbances
Max. error of *e*	1.9 *rad/s*	4.6 *rad/s*	9 *rad/s*
RMS error of *e*	0.4 *rad/s*	0.5 *rad/s*	2.1 *rad/s*

Chebyshev NN control system has smaller tracking errors with respect to the PI controller at three test cases. According to the tabulated measurements, the proposed hybrid recurrent Chebyshev NN control system indeed yields the superior control performance than the PI controller.

5. Conclusion

The hybrid recurrent Chebyshev NN control system has been successfully developed to control the V-belt CVT system, which is driven by PMSM. First, the dynamic models of the V-belt CVT system driven by PMSM were derived. Since the V-belt CVT system driven by PMSM is a nonlinear and time-varying system, sluggish speed is obtained for V-belt CVT system driven by PMSM using the PI controller due to the weak robustness of the linear controller. Therefore, to ensure the better control performance, the hybrid recurrent Chebyshev NN control system is developed to control the V-belt CVT system driven by PMSM under the occurrence of the lumped nonlinear external disturbances and the parameters variation.

The hybrid recurrent Chebyshev NN control system with inspected control based on the uncertainty bounds of the controlled system was designed to stabilize the system states around a predetermined bound area. To drop the excessive and chattering resulted by control efforts, the hybrid recurrent Chebyshev NN control system, which is composed of the inspected control, the recurrent Chebyshev NN control with adaptive law and the recouped control, was proposed to reduce and smooth the control effort when the system states were inside the predetermined bound area.

Moreover, online parameters tuning method of the recurrent Chebyshev NN control system with optimal learning rate is used based on Lyapunov stability theorem and the gradient descent method to increase the online learning capability of the recurrent Chebyshev NN. From the experimental results, the control performance of the proposed hybrid recurrent Chebyshev NN control system is more suitable than the PI controller for the V-belt CVT system driven by PMSM.

Acknowledgements

The author would like to acknowledge the financial support of the Ministry of Science and Technology in Taiwan. through its grant MOST 103-2221-E-239 -016.

References

[1] C. Y. Tseng, L. W. Chen, Y. T. Lin and J. Y. Li, "A hybrid dynamic simulation model for urban scooters with a mechanical-type CVT," *in IEEE Int. Conf. Automation and Logistics,* 2008, pp. 519-519.

[2] C. Y. Tseng, Y. F. Lue, Y. T. Lin, J. C. Siao, C. H. Tsai and L. M. Fu, "Dynamic simulation model for hybrid electric scooters," *in IEEE Int. Symp. Industrial Electronics*, 2009, pp. 1464-1469.

[3] L. Guzzella and A. M. Schmid, "Feedback linearization of spark-ignition engines with continuously variable transmissions," *IEEE Trans. Contr. Syst. Technol.*, vol. 3, no. 1, pp. 54-58, Mar. 1995.

[4] W. Kim and G. Vachtsevanos, "Fuzzy logic ratio control for a CVT hydraulic module," in *Proc. IEEE Symp. Intelligent Control*, 2000, pp. 151–156.

[5] D. W. Novotny and T. A. Lipo, *Vector Control and Dynamics of AC Drives*, NY: Oxford University Press, 1996.

[6] W. Leonhard, *Control of Electrical Drives*, Berlin: Springer-Verlag, 1996.

[7] F.J. Lin, "Real-time IP position controller design with torque feedforward control for PM synchronous motor," *IEEE Trans. Industrial Electronics*, vol. 4, no. 2, pp. 398-407, Mar. 1997.

[8] S. Haykin, *Neural Networks*, Ottawa, ON, Canada: Maxwell Macmillan, 1994.

[9] P. S. Sastry, G. Santharam, and K. P. Unnikrishnan, "Memory neural networks for identification and control of dynamical systems," *IEEE Trans. Neural Networks*, vol. 5, no. 2, pp. 306-319, Mar. 1994.

[10] R. Grino, G. Cembrano, and C. Torras, "Nonlinear system identification using additive dynamic neural networks – two on-line approaches," *IEEE Trans.*

Circuits and Systems I, vol. 47, no. 2, pp. 150-165, Feb. 2000.
[11] W. Huang, S. K. Oh, and H. Zhang, "Multiobjective space search optimization and information granulation in the design of fuzzy radial basis function neural networks," *J. Elect. Eng. Technol.,* vol. 7, no. 4, pp. 636-645, July 2012.
[12] K. S. Narendra and K. Parthasarathy, "Identification and control of dynamical systems using neural networks," *IEEE Trans. Neural Networks*, vol. 1, no. 1, pp. 4-26, Mar. 1990.
[13] D. H. Nguyen and B. Widrow, "Neural networks for self-learning control system," *IEEE Control System Magazine*, vol. 10, no. 3, pp.18-23, Apr. 1990.
[14] M. N. Eskander, "Minimization of losses in permanent magnet synchronous motors using neural network," *J. Power Electronics*, vol. 2, no. 3, pp. 220-229, July 2002.
[15] D. Q. Dang, N. T. T. Vu, H. H. Choi, and J. W. Jung, "Neuro-fuzzy control of interior permanent magnet synchronous motors: stability analysis and implementation," *J. Elect. Eng. Technol.,* vol. 8, no. 6, pp. 1439-1450, Nov. 2013.
[16] Namatame and N. Ueda, "Pattern classification with Chebyshev neural networks," *Int. J. Neural Networks,* 3 (1), pp. 23-31, 1992.
[17] T.T. Lee and J. T. Jeng, "The Chebyshev polynomial-based unified model neural networks for functional approximation," *IEEE Trans. System, Man and Cybernetics B*, vol. 28, no. 6, pp. 925-935, Dec. 1998.
[18] M. F. Moller, "A scaled conjugate gradient algorithm for fast supervised learning," *Neural Networks*, vol. 6, no. 4, pp. 525-533, 1993.
[19] R. Battiti, "First- and second-order methods for learning: Between steepest descent and Newton's method," *Neural Computation*, vol. 4, no. 2, pp. 141-166, Mar. 1992.
[20] C. Charalambous, "Conjugate gradient algorithm for efficient training of artificial neural networks," *Proc. Inst. Electric Engineering G*, vol. 139, no. 3, pp. 301-310, June 1992.
[21] M. T. Hagan and M. B. Menhaj, "Training feed-forward networks with Marquardt algorithm," *IEEE Trans. Neural Networks*, vol. 5, no. 6, pp. 989-993, Nov. 1994.
[22] R.K. Madyastha and B. Aazhang, "An algorithm for training multilayer perceptrons for data classify-cation and function interpolation," *IEEE Trans. Circuits and Systems I*, vol. 41, no. 12, pp. 866-875, Dec. 1994.
[23] T. W. S. Chow and Y. Fang, "A recurrent neural-network-based real-time learning control strategy applying to nonlinear systems with unknown dynamics," *IEEE Trans. Industrial Electronics*, vol. 45, no. 1, pp. 151-161, Feb. 1998.
[24] M. A. Brdys and G. J. Kulawski, "Dynamic neural controllers for induction motor," *IEEE Trans. Neural Networks*, vol. 10, no. 2, pp. 340-355, Mar. 1999.
[25] X.D. Li, J.K.L. Ho, and T.W.S. Chow, "Approximation of dynamical time-variant systems by continuous-time recurrent neural networks," *IEEE Trans. Circuits and Systems* II, vol. 52, no. 10, pp. 656-660, Oct. 2005.
[26] C. H. Lu and C. C. Tsai, "Adaptive predictive control with recurrent neural network for industrial processes: an application to temperature control of a variable-frequency oil-cooling machine," *IEEE Trans. Industrial Electronics*, vol. 55, no. 3, pp. 1366-1375, Mar. 2008.
[27] F. Payam, M. N. Hashemnia, J. Faiz, "Robust DTC control of doubly-fed induction machines based on input-output feedback linearization using recurrent neural networks," *J. Power Electronics*, vol. 11, no. 5, pp. 719-725, Sep. 2011.
[28] C. H. Lin and C. P. Lin, "The hybrid RFNN control for a PMSM drive system using rotor flux estimator," *Int. J. Power Electronics*, vol. 4, no. 1, pp. 33-48, 2012.
[29] C. H. Lin, P. H. Chiang, C. S. Tseng, Y. L. Lin, and M. Y. Lee, "Hybrid recurrent fuzzy neural network control for permanent magnet synchronous motor applied in electric scooter," in 6^{th} *Int. Power Electronics Conference*, 2010, pp. 1371-1376.
[30] C. H. Lin, "Hybrid recurrent wavelet neural network control of PMSM servo-drive system for electric scooter," *Int. J. Automatic Control Systems,* vol. 12, no. 1, pp. 177-187, Feb. 2014.
[31] K. J. Astrom and T. Hagglund, *PID Controller: Theory, Design, and Tuning,* North Carolina: Instrument Society of America, Research Triangle Park, 1995
[32] T. Hagglund and K. J. Astrom, "Revisiting the Ziegler- Nichols tuning rules for PI control," *Asian J. Control,* vol. 4, no. 4, pp. 364-380, Dec. 2002.
[33] T. Hagglund and K.J. Astrom, "Revisiting the Ziegler-Nichols tuning rules for PI control — part II: the frequency response method," *Asian J. Control,* vol. 6, no. 4, pp. 469-482, Dec. 2004.
[34] J. J. E. Slotine and W. Li, *Applied Nonlinear Control*, Englewood Cliffs, NJ: Prentice-Hall, 1991.
[35] K. J. Astrom and B. Wittenmark, *Adaptive Control*, NY: Addison-Wesley, 1995.

Chih-Hong Lin received his B.S. and M.S. in Electrical Engineering for National Taiwan University of Science and Technology, Taipei, Taiwan, R.O.C., in 1989 and 1991, respectively. He received his Ph. D. in Electrical Engineering from Chung Yuan Christian University, Chung Li, Taiwan, R.O.C., in 2001. He is currently an associate Professor in the electrical engineering, National United University, Miao Li, Taiwan, R.O.C. His research interests include power electronics, motor servo drives and intelligent control.